Desalination and Water Treatment
www.deswater.com

doi: 10.5004/dwt.2018.21658

101 (2018) 45–52
January

Combined effect of scale-forming ions and humic acid on nanofiltration membrane fouling

Jihyeok Choi[a], Yongjun Choi[a], Sangho Lee[a,*], Juneseok Choi[b]

[a]*School of Civil and Environmental Engineering, Kookmin University, Jeongneung-Dong, Seongbuk-Gu, Seoul, 136-702, Korea, Tel. 82 2 910 4529; Fax: 82 2 910 4939; emails: sanghlee@kookmin.ac.kr (S. Lee), choiyj1041@gmail.com (Y. Choi)*
[b]*Korea Institute of Construction Technology, 1190, Simindae-Ro, Ilsanseo-Gu, Goyang-Si, Gyeonggi-Do, Korea, email: jschoi@kict.re.kr*

Received 27 August 2017; Accepted 28 October 2017

ABSTRACT

In this study, a model for the progress of membrane fouling due to scale formation in nanofiltration systems is presented. The model was developed based on the surface blockage equation to estimate flux as a function of volume concentration factor (VCF). Experiments were carried out to apply the model using $CaSO_4$ saturated solution. Humic acid was used as a background organic matter that may interfere with the scale formation. The model could match the experimental data well with the overall R^2 value of 0.95 for more than 1,000 data points. The addition of the humic acid affected the changes in flux with VCF. The model parameters were different for different humic acid concentration. It is likely that the humic acid retards the scale formation rate by changing the crystallization kinetics. The rate of flux decline and VCF increase were also estimated as a function of the humic acid concentration.

Keywords: Desalination; Scale formation; Humic acid; Fouling; Model; Nanofiltration

1. Introduction

Nanofiltration (NF), which uses membranes less tight than reverse osmosis (RO) membrane, has been considered as an efficient technique for water treatment and desalination [1]. NF membranes have the capability of selective removal of divalent ions and dissolved organic matter, allowing their use for water softening [2,3]. They are also useful to reject emerging contaminants in water [4,5]. Recent development of novel NF membrane materials has broadened the application area for NF processing [6]. NF has been already proven to be sufficient to produce clear water in a variety of applications [1,7]. It has been also applied as a low-cost desalination technology [8].

Nonetheless, one of the challenges to be overcome for the application of NF is the control of membrane fouling [7,9,10]. Of particular importance in the water softening by NF is scale formation [11,12]. The hardness of water results from the existence of calcium and magnesium ions that can also cause scale formation in NF processing [13]. Once scale formation occurs, it can induce the formation of impermeable inorganic materials on the surface of membranes, leading to a reduction in the permeability of the membrane [11].

Due to the importance of scale formation issues in NF processing, a handful of studies have been carried out to understand and control scales [14–17]. The mechanisms of scale formation in NF/RO systems have been investigated [18]. Two scale formation mechanisms including surface crystallization and bulk crystallization have been reported [19]. A theoretical and experimental approach to estimate the potential for scale formation in RO and NF systems was also presented [14,20]. The interactions between scale-forming ions and dissolved chemicals in the water were examined [9,11,13,21]. It was found that the organic matters such as humic substances affect the kinetics of scale formation, which change flux decline rate in NF/RO systems. However,

* Corresponding author.

inorganic scaling was found to be accelerated by the organic fouling layer depending on the operating conditions [22]. The techniques for the measurement of NF membrane fouled by sparingly soluble salt have been developed and applied [23].

However, there is still limited information on the prediction of NF fouling due to scale formation. Models to predict the formation of scales in NF processing are highly required to achieve reliable design and operation of the membrane plants. Moreover, the effect of background organic matters such as humic acid on NF fouling should be further elucidated to apply NF in practical situations where both scale-forming ions and hardness exist.

In this study, a mechanistic modeling technique to quantify $CaSO_4$ scaling in NF membrane processing was developed. Using this technique, the possible influence of humic acid on scale formation in the NF system was analyzed. The originality of this work lies in the development of model allowing the analysis of NF fouling induced by both $CaSO_4$ and humic acid, which may provide insight into the design and operation of NF plants under similar situations.

2. Model development

The approach in this study was based on the resistance models for NF and surface crystallization kinetic equations. Although bulk crystallization may occur depending on the operating conditions, it was not considered in this model due to its relatively low effect in a bench-scale batch system, which was adopted in this study [12,21]. Accordingly, the flux is given by the following equation:

$$J = \frac{\left(\Delta P - \Delta\pi\right)}{\eta R_m}\left(\frac{A - A_b}{A}\right) = J_0\left(1 - \frac{A_b}{A}\right) \tag{1}$$

where J is the water flux through the NF membrane, ΔP is the difference between feed and permeate pressures; $\Delta\pi$ is the difference in osmotic pressure between feed and permeate; η is the viscosity of product water; R_m is the intrinsic resistance of intact membrane; A is the area of the membrane; A_b is the area blocked by surface crystals. Since the thickness of the surface crystal (h) is assumed to be constant, A_b can be expressed as:

$$A_b = \frac{m_s}{\rho h} = \beta m_s \tag{2}$$

where m_s is the mass of scales precipitated on the membrane surface; ρ is the density of the crystal and β is the coefficient for the surface crystal property. Since $J_0 = \Delta P/\eta R_m$, Eq. (1) is rewritten as

$$J_r = \frac{J}{J_0} = 1 - \frac{m_s}{\rho h A} = 1 - \frac{\beta m_s}{A} \tag{3}$$

where J_r is the reduced (or normalized) flux. According to Eq. (3), J_r linearly decreases as m_s increases. In fact, m_s is a function of the concentration of the scale-forming ions. Based on the kinetics for the crystal growth, m_s is given by:

$$m_s = \int_0^t k'\left(A - A_b\right)\left(c - c_s\right)^l \mathrm{d}t \tag{4}$$

where k' is the rate constant of the surface crystal growth; c is the scale-forming ion concentration; c_s is the scale-forming ion concentration at which the scale formation begins; l is the reaction order and t is the time. If there is no lag period for crystallization, c_s should be identical to the saturated concentration. However, due to the lag period, c_s may be higher than the saturated concentration. Since the aim of this study was to derive a semi-empirical model, m_s is simply given by:

$$m_s = k_s\left(c - c_s\right)^n \tag{5}$$

where k_s is the apparent rate constant of the surface crystal growth and n is the apparent reaction order. Using $x = c/c_0$ and $x_s = c_s/c_0$, Eq. (3) is rewritten by:

$$J_r = 1 - \frac{k\beta c_0}{A}\left(\frac{c}{c_0} - \frac{c_s}{c_0}\right)^n \approx 1 - \gamma\left(x - x_s\right)^n \tag{6}$$

where c_0 is the initial concentration of the scale-forming ions and γ is the apparent rate constant for flux decline. In the application of the model, Eq. (6) was used to fit the experimental results through non-linear regression to find the three parameters including γ, x_s and n.

3. Experimental

3.1. Experimental methods

A batch filtration cell was adopted to estimate filterability of NF membranes [21]. The composing material of the filtration cell was stainless steel. The filtration cell with the inner diameter of 54 mm was used. A magnetic stirrer with the size of 52 mm was applied to provide a proper mixing condition. The stirring speed was set to be 600 rpm, which corresponds to the shear rate of 6,920 s^{-1}. Transmembrane pressure (TMP) was adjusted using a high pressure regulator connected to a high pressure gas tank. Experiments were carried out at 6 and 12 bar, respectively. The feed temperature was set to 20°C–25°C. During the tests, the variations of the temperature during an experiment were smaller than ±1°C.

3.2. Feed water and membrane

A solution of 2,000 mg/L $CaSO_4$ was used as the feed to the NF system. Pre-filtration of the feed solutions was carried out using a 0.45 μm microfilter. During the experiments, the concentrations of $CaSO_4$ were determined using an electric conductivity meter. Humic acid (Sigma-Aldrich, USA) purchased from Sigma-Aldrich Chemical was used as a background organic matter. It was dissolved in water without further purification and the stock solutions were prepared. They were stored in a refrigerator at 4°C before use. The concentration of humic acid was determined using a Dohrmann DC-180 TOC Analyzer.

A commercially available thin film composite membrane (NF-45, Filmtec, USA) was selected for the NF experiments. The water permeability ranges from 6 to 7 L/m^2 h bar with the $CaSO_4$ rejection of 98%. A new membrane was used in each test. Before the test, the membranes were washed using the ultrapure water. The permeate flux was expressed in terms

of volume concentration factor (VCF), which is the ratio between the feed volume and the concentrate volume:

$$\mathrm{VCF} = \frac{V_f}{V_c} = 1 + \frac{V_p}{V_c} \tag{7}$$

where V_f, V_c and V_p are the volumes of feed, concentrate and permeate, respectively. VCF is proportional to permeate recovery.

The rate of flux decline was quantitatively expressed using the rate of flux decline (r_{FD}), which is defined as:

$$r_{FD} = \frac{J_i - J_f}{\Delta t} \tag{8}$$

where J_i is the initial water flux; J_f is the final water flux after the experiment and ΔT is the time spent during the experiment. While r_{FD} indicates how fast the flux decline occurs, it is also necessary to examine how fast the feed solution is concentrated. Accordingly, the rate of VCF increase was also measured by using the following equation:

$$r_{CF} = \frac{x_f}{\Delta t} \tag{9}$$

where x_f is the final VCF. The effect of humic acid concentration and the TMP on r_{FD} and r_{CF} was examined through a set of experiments.

4. Results and discussion

4.1. Effect of scale formation on NF flux

A set of NF tests were carried out by adjusting the concentration of humic acid from 0 to 10 mg/L in the $CaSO_4$ saturated solutions. The tests were done under low TMP (6 bar) and high TMP (12 bar). The experimental matrix is summarized in Table 1. In each case, the flux data were fitted to Eq. (6) to determine γ, x_s and n. If humic acid affects the NF fouling due to scale formation, these parameters may be changed.

Table 1
Experimental matrix

Transmembrane pressure (bar)	Humic acid concentration (mg/L)
12	0
12	0.2
12	0.4
12	0.6
12	0.8
12	1
12	2
12	4
6	0
6	0.5
6	1
6	2
6	10

Fig. 1(a) shows the results of NF test under 12 bar without adding the humic acid. The symbols denote the experimental values and the curve indicates the model fit. The NF flux gradually decreased from the beginning and was rapidly reduced above the VCF of 5, which results from the scale formation and subsequent fouling. The final VCF at the end of the experiment was about 6.3. The model reflects the overall tendency of flux decline during the experiments. The model fit parameters were determined as follows: γ = 0.0337, x_s = 1.34 and n = 2.11.

The existence of humic acid in the NF feed seems to retard the fouling by scaling. In Fig. 1(b), where the humic acid concentration was 0.2 mg/L, the flux decline pattern was similar to that without humic acid. However, with increased humic acid concentration, the flux decline was delayed. For example, Figs. 1(c) and (d) show the results at 0.4 and 0.6 mg/L of the humic acid concentrations, respectively. In these cases, the final VCF was approximately 7.0, which is higher than that without humic acid. If the humic acid concentration is higher than 1.0 mg/L (Figs. 1(f)–(h)), the final VCF was over 8.0, indicating that the fouling rate was reduced. Although there were some deviations, it is likely that the humic acid disturbs the fouling due to scale formation. Table 2 summarizes the results of model fits at high TMP condition. The γ value ranges from 0.0314 to 0.109 and the n ranges from 0.826 to 2.25. The x_s was in the range of 1.00 to 1.34. Although there are variations in the results, an increased concentration of the humic acid seems to reduce the n value. On the other hand, there were no evident trends between the humic acid concentration and the γ value. Moreover, the x_s seems to be almost constant in most cases.

Fig. 2(a) shows the results of NF test at 6 bar without adding the humic acid. Unlike the case with 12 bar (Fig. 1(a)), the flux linearly decreased with an increase in VCF. It appears that the fouling due to scale formation started from the beginning of the experiment. Nevertheless, the model provides a reasonable agreement with the experimental data. The model fit parameters were estimated as: γ = 0.3130, x_s = 1.00 and n = 0.680. Compared with the case with 12 bar, the n value was lower, indicating that the apparent reaction order was reduced. This suggests that the kinetics of scale formation at 6 and 12 bar are quite different.

With an increase in the humic acid concentration, the flux decline rate was reduced. In Fig. 2(b) the final VCF was 7.9, which is higher than the final VCF without humic acid. The final VCF increased to 10 if the concentration of humic acid was higher than 1 mg/L (Figs. 2(c)–(e)). The slope of the flux decline also decreased with an increase in the humic acid concentration. At the humic acid concentration of 10 mg/L (Fig. 2(e)), the reduced flux was still 0.4 even at the end of the NF test. The changes in flux with time were successfully described by the model.

The results of model fits at low TMP condition are presented in Table 3. The γ value ranges from 0.242 to 0.313 and the n value ranges from 0.680 to 334. The x_s was close to 1.00 in most cases. It seems that the existence of humic acid does not significantly affect the γ and x_s values. However, it showed a strong correlation with the n value. It is evident that n decreased as an increase in the humic acid concentration.

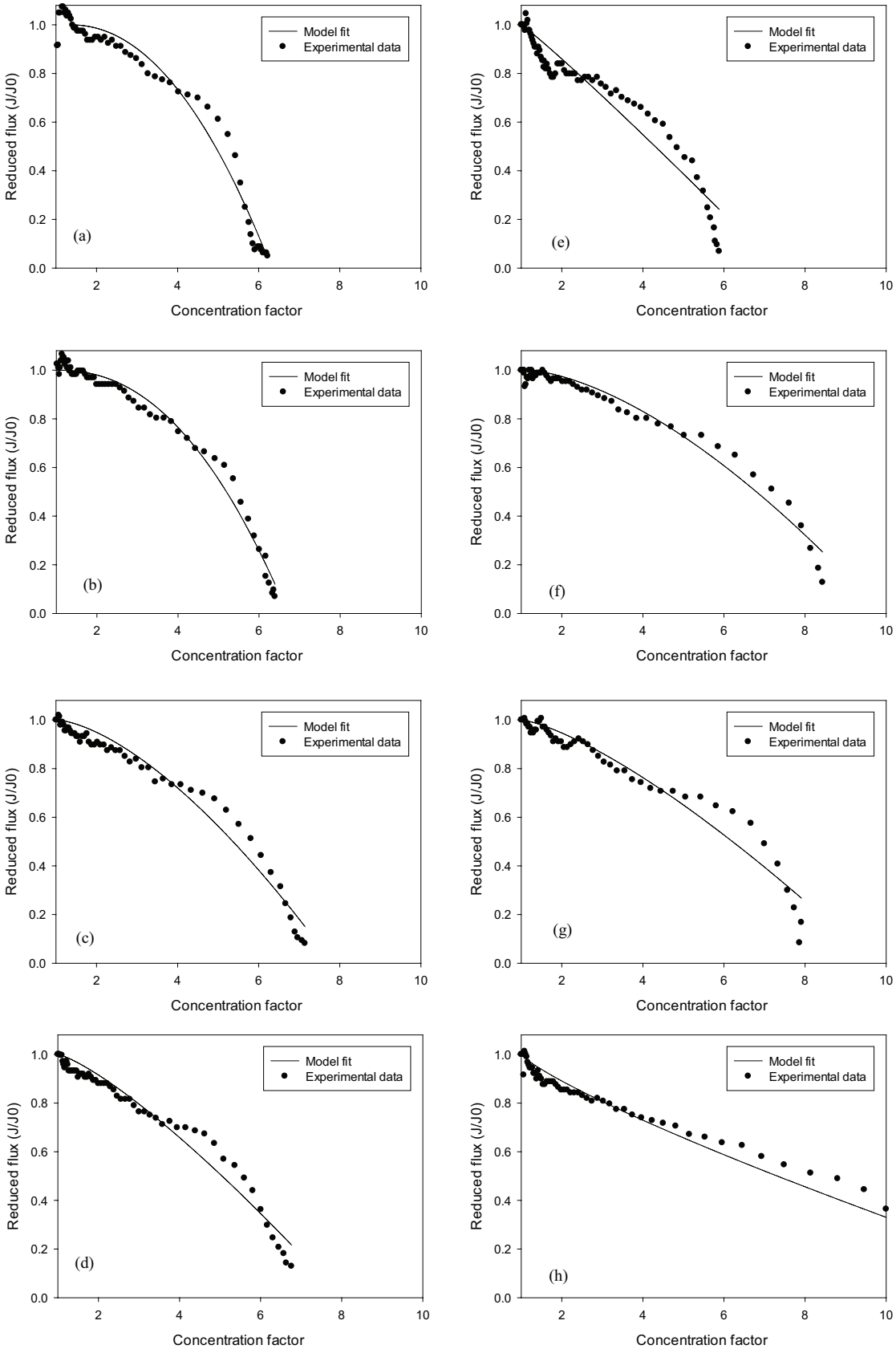

Fig. 1. Dependence of the reduced flux on VCF at TMP of 12 bar. Humic acid concentrations: (a) 0, (b) 0.2, (c) 0.4, (d) 0.6, (e) 0.8, (f) 1.0, (g) 2.0 and (h) 4.0 mg/L.

The dependence of γ and *n* on humic acid concentration is illustrated in Fig. 3. When the TMP was 6 bar, the γ remains constant irrespective of the humic acid concentration, as shown in Fig. 3(a). At the TMP of 12 bar, the γ seems to increase with the concentration of the humic acid. However, due to the variations of the data, it is not clear if the γ really depends on the humic acid concentration. On the other hand, the *n* is strongly dependent on the humic acid concentration as shown in Fig. 3(b). Accordingly, it can be concluded that the retardation of scale formation by humic acid in the NF system is attributed to the modification of crystallization kinetics due to the interaction between $CaSO_4$ salts and humic acid.

Table 2
Model fit parameters at high TMP conditions (12 bar)

Humic acid concentration (mg/L)	Model parameters		
	γ	x_s	*n*
0	0.0337	1.34	2.11
0.2	0.0199	1.00	2.25
0.4	0.0508	1.00	1.55
0.6	0.0846	1.00	1.27
0.8	0.140	1.00	1.064
1	0.0314	1.12	1.59
2	0.0536	1.00	1.35
4	0.109	1.00	0.826

Table 3
Model fit parameters at low TMP conditions (6 bar)

Humic acid concentration (mg/L)	Model parameters		
	γ	x_s	*n*
0	0.3130	1.00	0.680
0.5	0.242	1.00	0.689
1	0.286	1.03	0.526
2	0.289	1.01	0.391
10	0.278	1.04	0.334

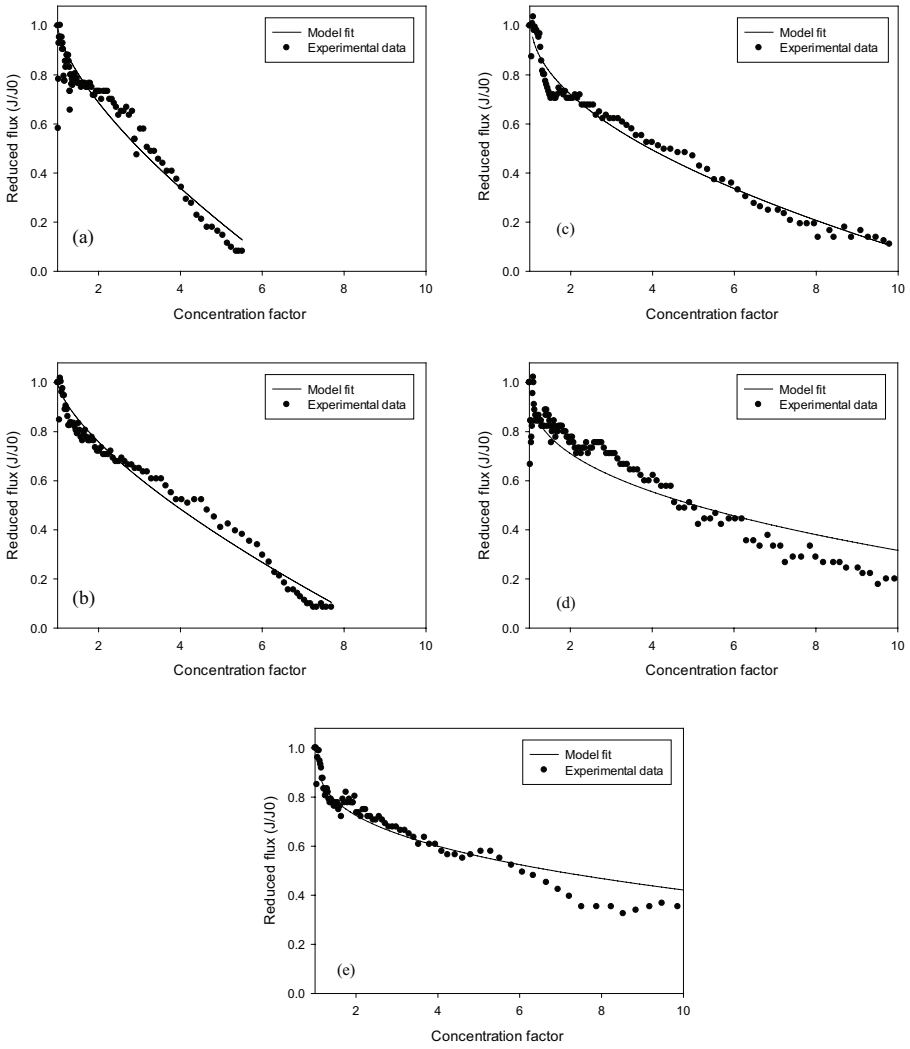

Fig. 2. Dependence of the reduced flux on VCF at TMP of 6 bar. Humic acid concentrations: (a) 0, (b) 0.5, (c) 1.0, (d) 2.0 and (e) 10.0 mg/L.

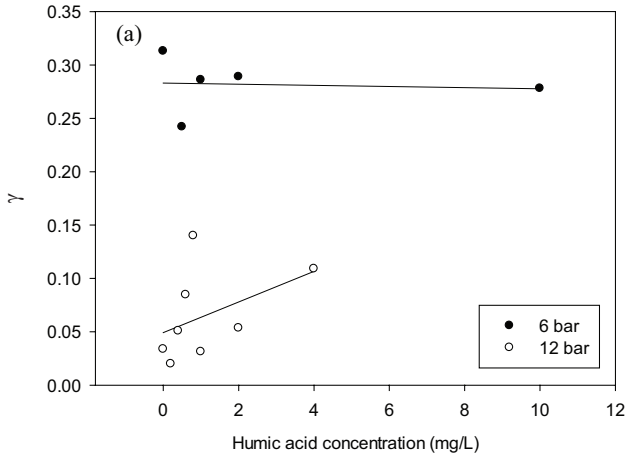

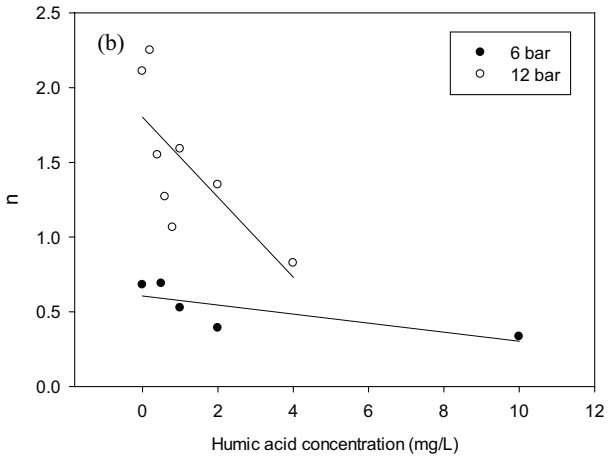

Fig. 3. Effect of humic acid concentration on model fit parameters (a) γ and (b) *n*.

4.2. Model verification

Fig. 4 shows the correlation between the experimental flux and the model calculations. Although there were some deviations, the model showed a good match with experiments. Except for the cases with low reduced flux, the model fits the experimental data well. The R^2 was 0.957 for 1,043 data points. This result suggests that the effect of humic acid on the fouling due to $CaSO_4$ scaling can be described by the simple model equation.

Although the model fit was successful, there were deviations in several cases. For example, the model fit in Fig. 1(e) does not seem to be adequate because the trends of the experimental results and the model fits are different. This is probably because of experimental errors occurred during the experiments. In Fig. 1(e), the flux in the initial phase was unstable, which affects the reliability of the model fit.

4.3. The rates of flux decline and VCF increase

Using Eqs. (8) and (9), r_{FD} and r_{CF} were calculated from the experimental data. In Fig. 5(a), the r_{FD} is shown as a function of

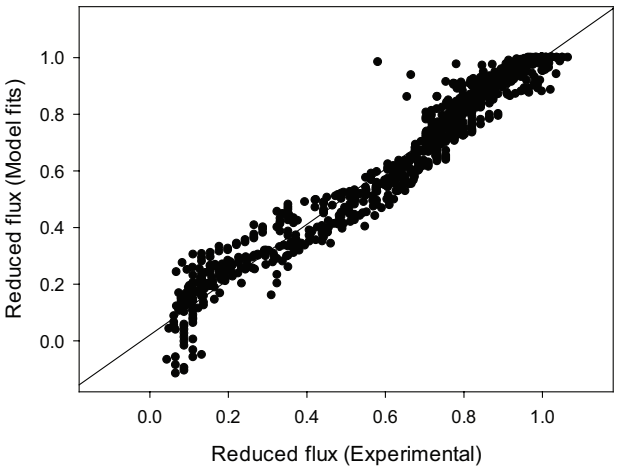

Fig. 4. Comparison of experimental data for reduced flux with model fits.

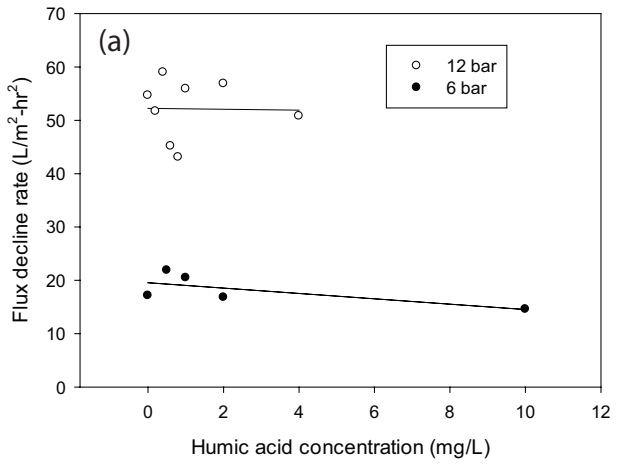

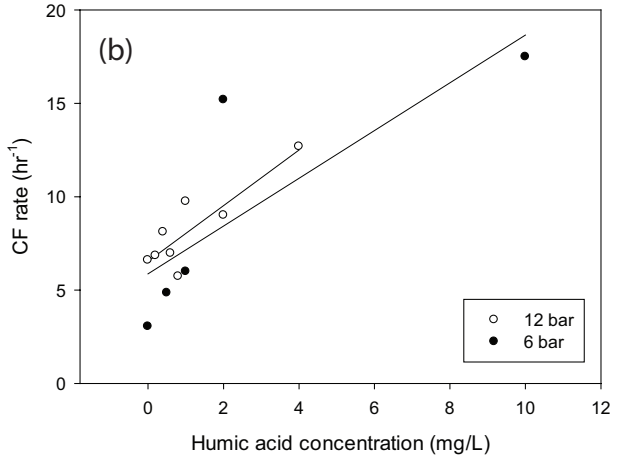

Fig. 5. Effect of humic acid concentration on the rates of flux decline and VCF increase (a) r_{FD} and (b) r_{CF}.

humic acid concentration for two TMP conditions. Considering the variations in the data, it is evident that r_{FD} does not depend on the humic acid concentration. The r_{FD} indicates the rate

Table 4
Dependence of r_{FD} and r_{CF} on TMP and humic acid concentration

Transmembrane pressure (bar)	Humic acid concentration (mg/L)	Flux decline rate, r_{FD} (L/m^2 h^2)	CF rate, r_{CF} (min^{-1})
12	0	54.7	6.60
12	0.2	51.7	6.85
12	0.4	59.0	8.11
12	0.6	45.2	6.97
12	0.8	43.1	5.74
12	1	55.9	9.76
12	2	56.9	9.02
12	4	50.8	12.7
6	0	17.15	3.05
6	0.5	21.9	4.85
6	1	20.5	6.00
6	2	16.8	15.2
6	10	14.6	17.5

of flux decline. If the humic acid exists, the flux decline is reduced by its retardation effect. However, it also leads to the NF operation at higher VCF and thus the flux decline eventually occurs. Accordingly, it seems that the r_{FD} does not significantly change in the presence of humic acid.

Fig. 5(b) shows r_{CF} as a function of the humic acid concentration. Unlike r_{FD}, r_{CF} seems to increase as an increase in the humic acid concentration. Since r_{CF} implies how fast the feed solution can be concentrated, it increases due the retardation of scale formation by the humic acid. In other words, the presence of humic acid is beneficial to produce more water from the feed water containing scale-forming ions. The results on r_{FD} and r_{CF} are summarized in Table 4.

Using the linear regression of the data in Fig. 5, r_{FD} and r_{CF} are expressed as a function of humic acid concentration and TMP. The regression equations were then used to create contour diagrams to show how r_{FD} and r_{CF} changes with the humic acid concentration and TMP. As shown in Fig. 6(a), r_{FD} is not significantly affected by the humic acid concentration. But it increases as the TMP increases. On the other hand, the effect of TMP on r_{CF} is not significant as shown in Fig. 6(b). Instead, an increase in the humic acid concentration increases r_{CF}. This suggests that the fouling by $CaSO_4$ scaling in NF systems is affected by the combined effect of humic acid concentration and TMP.

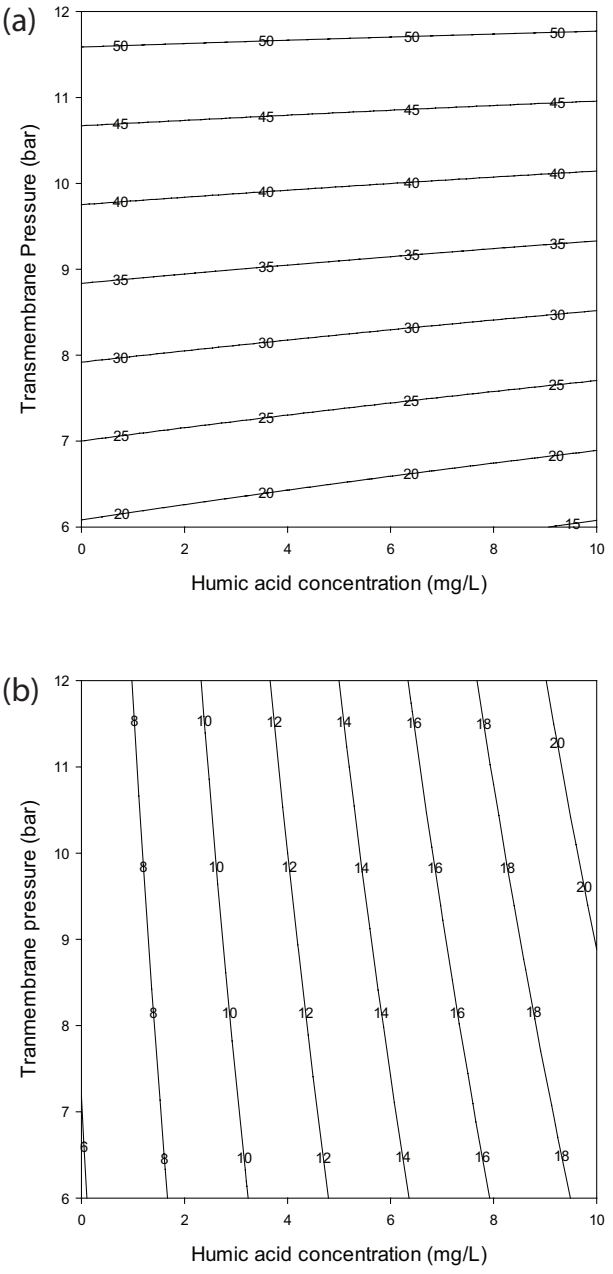

Fig. 6. Contours of the rates of flux decline and VCF increase as a function of humic acid concentration and TMP (a) r_{FD} and (b) r_{CF}.

5. Conclusion

In this study, NF fouling by $CaSO_4$ scaling in the presence of humic acid was investigated. The following conclusions were drawn:

- A model was developed based on the surface blockage equation to estimate flux as a function of VCF. The model could match the experimental data well with the overall R^2 value of 0.95 for more than 1,000 data points.
- The humic acid seems to retard the fouling by $CaSO_4$ scaling. With increasing the humic acid concentration, the final VCF obtained at the end of the experiments increases.
- The apparent reaction order (n) for the scale formation decreases with increasing the humic acid concentration. This suggests that the retardation of scale formation by humic acid in the NF system is attributed to the modification of crystallization kinetics due to the interaction between $CaSO_4$ and humic acid.
- The rate of flux decline (r_{FD}) did not depend on the humic acid concentration but the rate of VCF increase (r_{CF}) was proportional to the humic acid concentration. On the other hand, only r_{FD} was significantly affected by the TMP.

Acknowledgments

This research was supported by grants (17IFIP-B065893-05 and 17IFIP-B116951-02) from Industrial Facilities & Infrastructure Research Program funded by Ministry of Land, Infrastructure and Transport of Korean government.

References

[1] D.L. Oatley-Radcliffe, M. Walters, T.J. Ainscough, P.M. Williams, A.W. Mohammad, N. Hilal, Nanofiltration membranes and processes: a review of research trends over the past decade, J. Water Process Eng., 19 (2017) 164–171.
[2] A.W. Mohammad, Y.H. Teow, W.L. Ang, Y.T. Chung, D.L. Oatley-Radcliffe, N. Hilal, Nanofiltration membranes review: recent advances and future prospects, Desalination, 356 (2015) 226–254.
[3] J.V. Nicolini, C.P. Borges, H.C. Ferraz, Selective rejection of ions and correlation with surface properties of nanofiltration membranes, Sep. Purif. Technol., 171 (2016) 238–247.
[4] O.M. Rodriguez-Narvaez, J.M. Peralta-Hernandez, A. Goonetilleke, E.R. Bandala, Treatment technologies for emerging contaminants in water: a review, Chem. Eng. J., 323 (2017) 361–380.
[5] J. Garcia-Ivars, L. Martella, M. Massella, C. Carbonell-Alcaina, M.-I. Alcaina-Miranda, M.-I. Iborra-Clar, Nanofiltration as tertiary treatment method for removing trace pharmaceutically active compounds in wastewater from wastewater treatment plants, Water Res., 125 (2017) 360–373.
[6] Y. Ji, W. Qian, Y. Yu, Q. An, L. Liu, Y. Zhou, C. Gao, Recent developments in nanofiltration membranes based on nanomaterials, Chin. J. Chem. Eng., 25 (2017) 1639–1652.
[7] S. Bunani, E. Yörükoğlu, G. Sert, Ü. Yüksel, M. Yüksel, N. Kabay, Application of nanofiltration for reuse of municipal wastewater and quality analysis of product water, Desalination, 315 (2013) 33–36.
[8] D. Zhou, L. Zhu, Y. Fu, M. Zhu, L. Xue, Development of lower cost seawater desalination processes using nanofiltration technologies—a review, Desalination, 376 (2015) 109–116.
[9] A.S. Al-Amoudi, Factors affecting natural organic matter (NOM) and scaling fouling in NF membranes: a review, Desalination, 259 (2010) 1–10.
[10] K. Listiarini, D.D. Sun, J.O. Leckie, Organic fouling of nanofiltration membranes: evaluating the effects of humic acid, calcium, alum coagulant and their combinations on the specific cake resistance, J. Membr. Sci., 332 (2009) 56–62.
[11] P. Dydo, M. Turek, J. Ciba, Scaling analysis of nanofiltration systems fed with saturated calcium sulfate solutions in the presence of carbonate ions, Desalination, 159 (2003) 245–251.
[12] S. Lee, J. Kim, C.-H. Lee, Analysis of $CaSO_4$ scale formation mechanism in various nanofiltration modules, J. Membr. Sci., 163 (1999) 63–74.
[13] N. Her, G. Amy, C. Jarusutthirak, Seasonal variations of nanofiltration (NF) foulants: identification and control, Desalination, 132 (2000) 143–160.
[14] R. Sheikholeslami, Assessment of the scaling potential for sparingly soluble salts in RO and NF units, Desalination, 167 (2004) 247–256.
[15] P. Dydo, M. Turek, J. Ciba, K. Wandachowicz, J. Misztal, The nucleation kinetic aspects of gypsum nanofiltration membrane scaling, Desalination, 164 (2004) 41–52.
[16] D. Almasri, K.A. Mahmoud, A. Abdel-Wahab, Two-stage sulfate removal from reject brine in inland desalination with zero-liquid discharge, Desalination, 362 (2015) 52–58.
[17] M. Shmulevsky, X. Li, H. Shemer, D. Hasson, R. Semiat, Analysis of the onset of calcium sulfate scaling on RO membranes, J. Membr. Sci., 524 (2017) 299–304.
[18] C.-J. Lin, S. Shirazi, P. Rao, S. Agarwal, Effects of operational parameters on cake formation of $CaSO_4$ in nanofiltration, Water Res., 40 (2006) 806–816.
[19] S. Lee, P.-K. Park, J.-H. Kim, K.-M. Yeon, C.-H. Lee, Analysis of filtration characteristics in submerged microfiltration for drinking water treatment, Water Res., 42 (2008) 3109–3121.
[20] Q. Huang, W. Ma, A model of estimating scaling potential in reverse osmosis and nanofiltration systems, Desalination, 288 (2012) 40–46.
[21] S. Lee, J.-S. Choi, C.-H. Lee, Behaviors of dissolved organic matter in membrane desalination, Desalination, 238 (2009) 109–116.
[22] J. Wang, L. Wang, R. Miao, Y. Lv, X. Wang, X. Meng, R. Yang, X. Zhang, Enhanced gypsum scaling by organic fouling layer on nanofiltration membrane: characteristics and mechanisms, Water Res., 91 (2016) 203–213.
[23] W. Hao, M. Yang, K. Zhao, J. Tang, Dielectric measurements of fouling of nanofiltration membranes by sparingly soluble salts, J. Membr. Sci., 497 (2016) 339–347.